PROCEEDINGS OF SCIENCE

Possible scenario of dynamical chiral symmetry breaking in the instanton liquid

Yamato Suda[a,*] **and Daisuke Jido**[a]

[a] *Department of Physics, Tokyo Institute of Technology,*
2-12-1 Ookayama, Meguro, Tokyo 152-8551, Japan

E-mail: suda.y.ad@m.titech.ac.jp, jido@th.phys.titech.ac.jp

Using simulations of the interacting instanton liquid model (IILM) with the flavor SU(3) symmetric quarks, we compute the free energy densify of the QCD vacuum as a function of the quark condensate. We then compute the second derivative of the free energy density with respect to the quark condensate at the origin. This computation allows us to investigate whether chiral symmetry breaking in the IILM occurs in an anomaly-driven manner. This chiral symmetry breaking pattern has been proposed in a previous study as a mechanism linking the QCD vacuum structure to meson properties, such as the mass of the sigma meson. We also perform quenched simulations, in which no dynamical quarks interact with instantons. Comparing these results with the full calculations provides a better understanding of chiral symmetry breaking patterns in the IILM. We find that in the full IILM, chiral symmetry is dynamically broken in anomaly-driven manner, whereas in the quenched IILM, it is broken through the ordinary mechanism. Based on these results, we would suggest that chiral symmetry breaking in real QCD might also occur in an anomaly-driven manner. Consequently, in phenomena where chiral symmetry breaking plays a crucial role, the anomalous effect may also have a significant impact.

The XVIth Quark Confinement and the Hadron Spectrum Conference (QCHSC24)
19-24 August, 2024
Cairns Convention Centre, Cairns, Queensland, Australia

*Speaker

 ISSN 1824-8039 . Published by SISSA Medialab.

PoS(QCHSC24)041

1. Introduction

The vacuum of strong interaction has a non-trivial structure, which leads characteristic phenomena such as color confinement and dynamical chiral symmetry breaking (DχSB). These phenomena are fundamental to the diversity of matter in the world. For example, due to color confinement, quarks cannot exist as elementary particles; instead, they form composite particles known as hadrons. As a result, hadrons exhibit a remarkable diversity, with hundreds of different types. Moreover, DχSB plays a crucial role in the generation of their mass. The total mass of current quarks accounts for less than 1% of the nucleon mass, while the remaining 99% is believed to arise from non-perturbative mechanism associated with DχSB.

The non-Abelian nature of quantum chromodynamics (QCD) results a topological structure that has a significant impact on hadron physics. QCD is formulated based on a non-Abelian gauge group, which allows the gauge fields to interact with themselves. As a result, Euler–Lagrange equations admit a purely topological, non-perturbative solution known as an instanton, even at the classical level [1]. This topological aspect of the QCD vacuum manifests itself as the axial anomaly—the breaking of $U(1)_A$ symmetry due to the quantum fluctuations [2, 3]. The axial anomaly, mediated by quark-antiquark correlations, significantly affects hadron physics [4, 5].

Recently, the authors in Ref. [6] discussed the patterns of chiral symmetry breaking and its consequences on the hadron spectra based on specific model parameters. They calculated the effective potential of the system and the hadron masses using the three-flavor Nambu–Jona-Lasinio (NJL) model and the linear sigma model, which includes the axial anomaly term, also known as the Kobayashi–Maskawa–'t Hooft (KMT) term [7]. In particular, in the NJL model, if the model parameter g_S, which is responsible for inter-quark attraction, is sufficiently strong ($g_S > g_S^{\rm crit}$), then chiral symmetry is dynamically broken in the vacuum, meaning that the effective potential takes its minimum at a finite quark condensate. We refer to this as the ordinary breaking. On the other hand, even when $g_S > g_S^{\rm crit}$, dynamical chiral symmetry breaking can still occur if a sufficiently large contribution from the axial anomaly exists. This is called anomaly-driven breaking. Furthermore, in the former case, if the mass of the sigma meson, which is the chiral partner of the pion, exceeds 800 MeV, whereas in the latter case, it remains below 800 MeV.

In this study, we investigate whether the scenarios of DχSB suggested in a previous study can occur in another model rather than in the models used in previous study. According to Ref. [6], the axial anomaly might play a significant role in the scenario of DχSB discussed there. Since the axial anomaly originates from topological fluctuations in the QCD vacuum, which are closely related to a classical solution to the Euclidean Yang-Mills equation, known as an instanton, we use the QCD vacuum model that respects the instanton degrees of freedom [8, 9]. Details of this study have already been published [11].

2. Dynamical chiral symmetry breaking driven by the axial anomaly

In this study, the criterion for identifying the pattern of DχSB in the vacuum is the sign of curvature, given by the second derivative of the vacuum energy density with respect to the quark

condensate at its origin $\langle \bar{q}q \rangle = 0$:

$$\left. \frac{\partial^2 \epsilon}{\partial \langle \bar{q}q \rangle^2} \right|_{\langle \bar{q}q \rangle = 0}. \tag{1}$$

Since the criterion used in the previous study is based on specific model parameters, it is not clear how it can be applied beyond those specific models. Therefore, we generalize the criterion as follows: If the curvature in Eq. (1) is positive, we identify this case as anomaly-driven chiral symmetry breaking, whereas if the curvature is negative, we conclude that chiral symmetry is dynamically broken in the ordinary manner. This procedure correctly reproduces the previous result when applied to the NJL model. We apply this criterion to simulations with finite current quark masses, while the original study fomulated the criterion in the chiral limit. We have confirmed that this criterion remains valid slightly way from the chiral limit.

3. Methodology

3.1 Partition function of the interacting instanton liquid model

We use the partition function of the interacting instanton liquid model (IILM) in the Euclidean space-time given by [16]:

$$Z = \frac{1}{N_+! N_-!} \int \prod_{i=1}^{N_+ + N_-} d\Omega_i f(\rho_i) e^{-S_{\rm int}} \prod_{f=1}^{N_f} \det(i\gamma^\mu D_\mu + m_f), \tag{2}$$

where the number of instantons (antiinstantons) inside the four volume V_4 is denoted by $N_{+(-)}$. The path integral measure $d\Omega$ includes the size, color orientation, and position of the i-th instantons, where $d\Omega_i = d\rho_i dU_i d^4 z_i$. The classical instanton amplitude $f(\rho_i)$ is a function of the instanton size ρ, which depends on the number of colors N_c and the number of flavors N_f [3]. The term $S_{\rm int}$ describes the instanton-instanton interaction [10], and D_μ represents the covariant derivative acting on a quark of flavor f and current mass m_f. For more details, including the explicit expression of $f(\rho)$ and $S_{\rm int}$, as well as the calculation strategy for the quark determinant, we refer the reader to Ref. [11].

In actual computations, we generate the flavor SU(3) symmetric IILM configurations, in which the quark masses for all flavors are set to $m_f = m$, using the partition function in Eq. (2) and employing the standard Hybrid Monte Carlo (HMC) and Metropolis methods [12–14]. For comparison, we also generate the quenched configurations, in which the quark determinant is omitted in Eq. (2), thereby excluding the instanton-quark interaction from the system. To simulate different instanton densities $n \equiv (N_+ + N_-)/V_4$, we generate the configurations while keeping $N_+ + N_- = 32$ fixed and varying the four-volume V_4.

3.2 Vacuum energy density

In this study, we use the free energy density, which is referred to simply as the free energy hereafter, to evaluate the curvature defined in Eq. (1). The free energy is given by

$$F = -\frac{1}{V_4} \ln Z. \tag{3}$$

According to the standard thermodynamics relation, this is identified as the vacuum energy density at zero temperature, $\epsilon = F$. Thus, we use the free energy to evaluate the curvature given in Eq. (1). To obtain F at a given density n, we need to calculate the partition function Z. In computing the partition function, we directly obtain its logarithm, $\ln Z$, where we employ the thermodynamic integration method described in detail in Refs. [5, 11]. Consequently, we obtain the value of F for a given instanton density n and a quark mass m, which characterize the configuration.

3.3 Quark condensate

We compute the quark condensate for a quark of flavor f with a current mass m_q as the expectation value of the traced quark propagator at the same coordinate:

$$\langle \bar{q}_f q_f \rangle = \sum_{A,\alpha} \langle q_f^\dagger(x)^A_\alpha q_f(x)^A_\alpha \rangle = -\lim_{y\to x} \frac{1}{Z} \int D\Omega \mathrm{Tr}[S(x,y;m_f)] e^{-S_{\mathrm{int}}} \det(\gamma^\mu D_\mu + m_f). \quad (4)$$

Here, the measure in the partition function in Eq. (2) is denoted by $D\Omega = \prod_i d\Omega_i$ for brevity. The indices A and α range from 1 to N_c and from 1 to 4, respectively. The trace operation is performed over both indices. We approximate the quark propagator by $S(x,y;m) \approx S_0(x,y) + S^{\mathrm{ZM}}(x,y;m)$ and consider only the zero-mode part of the second term, excluding the contribution from the free part, whose contribution diverges at the coincident coordinate.

3.4 Evaluation of the curvature

We evaluate the curvature by fitting the data to a polynomial [15]. After performing simulations over a wide range of the instanton densities n, we obtain data series for (n, F) and $(n, \langle \bar{q}q \rangle)$. For a given density n, the values of F and $\langle \bar{q}q \rangle$ are uniquely determined. Thus, we use the data series $(\langle \bar{q}q \rangle, F)$ to evaluate the curvature of the free energy with respect to the quark condensate. The polynomial model to evaluate the curvature is given by

$$F = \sum_{j=0}^{K} C_j \langle \bar{q}q \rangle^j , \quad (5)$$

where C_j represents the coefficient of the jth order term obtained from the fitting. We are interested in the sign of the curvature at the origin, which corresponds to the sign of the coefficient C_2. Thus, we focus on the value of C_2 in the following analysis.

4. Numerical Results

In the flavor SU(3) symmetric calculations, we perform computations for three different values of the current quark mass: $m = 37, 54$ and 70 MeV. Each simulation with a given current quark mass m is associated with a scale parameter Λ. This scale parameter is determined so that the free energy is minimized at the instanton density $n = 1$ fm^{-4}, following Ref. [16].

In Fig. 1, we show the dependence of the free energy on the instanton density for three different current quark masses. In regions where the density satisfies $n < 1$ fm^{-4}, the free energy decreases monotonically as the density increases. This indicates an attractive interaction between instantons

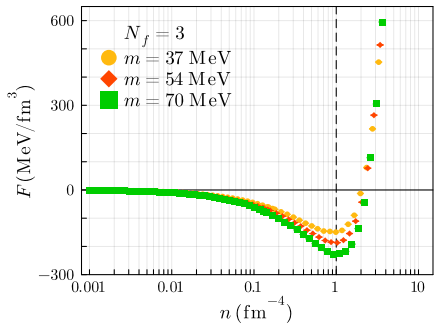

Figure 1: Free energy versus instanton density in the flavor SU(3) symmetric IILM. This figure is based on the work [11].

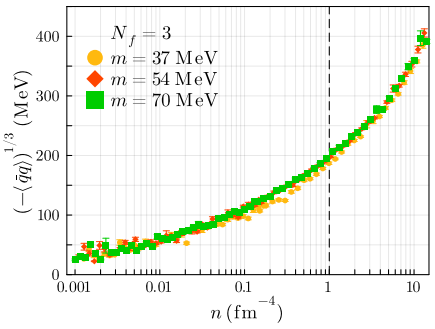

Figure 2: Quark condensate versus instanton density in the flavor SU(3) symmetric IILM. This figure is based on the work [11].

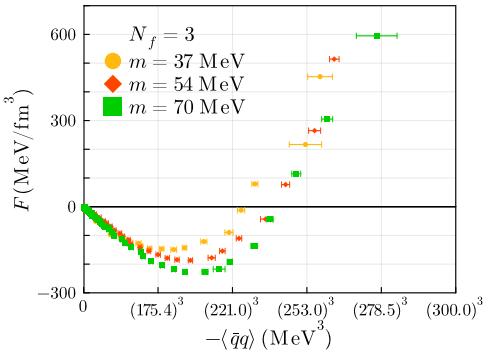

Figure 3: Free energy versus quark condensate in the flavor SU(3) symmetric IILM. This figure is based on the work [11].

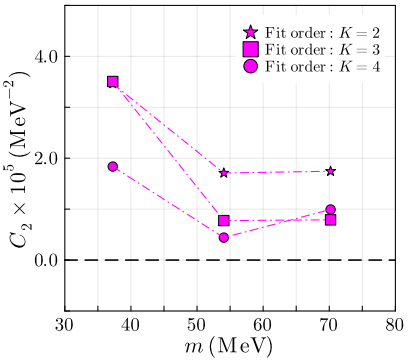

Figure 4: Coefficient C_2 in the flavor SU(3) symmetric IILM for different current quark masses. This figure is based on the work [11].

in a dilute regime. At the density $n = 1$ fm^{-4}, the free energy reaches its minimum by definition. At high densities, the free energy increases rapidly, indicating a repulsive interaction.

In Fig. 2, we show the magnitude of the quark condensate versus the instanton density for three different current quark masses. We observe that at the vacuum instanton density, i.e., $n = 1$ fm^{-4}, the quark condensate takes nearly the same value, independent of the current quark mass. This suggests that explicit chiral symmetry breaking caused by the current quark mass is small compared to the dynamical breaking.

In Fig. 3, we show the free energy versus quark condensate, obtained by combining the results of (n, F) and $(n, \langle\bar{q}q\rangle)$. The free energy reaches its minimum at a finite vale of the quark condensate. This suggests that chiral symmetry is broken dynamically in the vacuum of the IILM.

In Fig. 4, we show the evaluation of C_2 for each current quark mass in the flavor SU(3) symmetric IILM. The coefficient C_2 remains positive, independent of the order of polynomial fitting and the current quark mass, even though its absolute value varies slightly. From this result, we conclude that the flavor SU(3) symmetric IILM exhibits the anomaly-driven chiral symmetry breaking.

For comparison, we performed the quenched simulations with three different current quarks

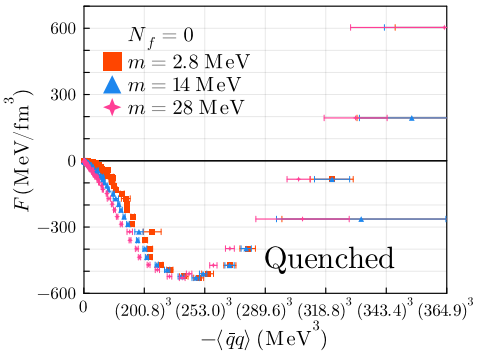

Figure 5: Free energy versus quark condensate. This figure is based on the work [11].

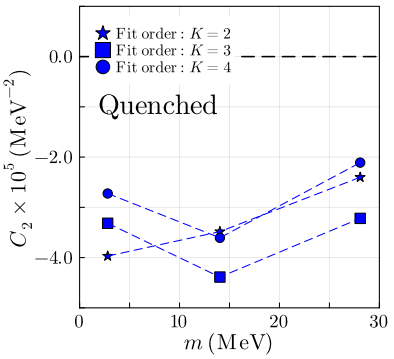

Figure 6: Coefficient C_2 for different current quark masses. This figure is based on the work [11].

masses: $m = 2.8$, 14 and 28 MeV, which are lighter than those used in the full calculations. In the quenched calculations, the current quark mass refers to the mass included in the quark propagator of Eq. (4). In Fig. 5, we present the plot of the free energy versus the quark condensate, obtained in a similar manner. This result indicates that chiral symmetry is also dynamically broken in the vacuum for the quenched system.

Figure 6 illustrates the values of C_2 for each current quark mass in the quenched calculation. We observe that the curvature has a negative value. This result suggests that chiral symmetry is dynamically broken in the ordinary way when the system excludes the instanton-quark interaction is absent.

5. Conclusion

The realization of the anomaly-driven chiral symmetry breaking in the flavor SU(3) symmetric IILM can be understood as follows. We have defined the anomaly-driven breaking as a breaking pattern in which chiral symmetry is dynamically broken in the vacuum, and the curvature of the vacuum energy density at the origin, as given in Eq. (1), is positive. As investigated in the previous study [6], such a scenario occurs, for example, in the three-flavor NJL model, when the attractive interaction between quarks is not sufficiently strong, but the KMT term is sufficiently strong. The KMT term, which introduces the axial anomaly, is expressed as a six-quark interaction. This interaction can be understood as part of the 't Hooft vertex in the three-flavor case [17]. In the context of the IILM, the 't Hooft vertex is incorporated into the quark determinant in Eq. (2). Therefore, full calculations that properly account for the quark determinant inherently include the 't Hooft vertex. Consequently, it is natural to interpret that the IILM with three-flavor quarks exhibits the anomaly-driven chiral symmetry breaking.

The results of the quenched calculations support this interpretation. In the quenched approximation, the quark determinant is set to unity, effectively suppressing the effects of the instanton-quark interaction. As a consequence, the interaction corresponding to the six-quark KMT term is absent, and the anomaly-driven chiral symmetry breaking does not occur. This absence of the instanton-quark interaction manifests as a negative curvature, $C_2 < 0$, in the quenched calculation.

6. Outlook

Currently, we are interested in two directions for further developing our work. The first is the investigation of chiral symmetry breaking patterns in intermediate flavor regimes, such as $N_f = 2$ and $N_f = 2 + 1$. When considering three quark flavors, a six-quark interaction like the KMT term arises but does not appear for $N_f = 0, 1$ or 2. The second direction is to examine whether the consequences of the anomaly-driven chiral symmetry breaking can also be reproduced in the IILM. The previous study concluded that the sigma meson, as the chiral partner of the pion, becomes lighter than approximately 800 MeV. This investigation is crucial for linking the discussion based on the curvature sign of the free energy to actual physical observables.

7. Acknowledgements

This work by Y.S. is supported by JST SPRING, Grant No. JPMJSP2106. The work of D.J. was supported in part by Grants-in-Aid for Sicentific Reserach from JSPS (Grants No. JP21K03530, No. JP22H04917, and No. JP23K03427).

References

[1] A. Belavin, A. Polyakov, A. Schwartz, Y. Tyupkin, "Pseudoparticle Solutions of the Yang-Mills Equations," Phys. Lett. B **59** (1975) 85.

[2] G. 't Hooft, "Symmetry breaking through Bell–Jackiw anomalies," Phys. Rev. Lett. **37** (1976) 8.

[3] G. 't Hooft, "Computation of the quantum effects due to four-dimensional pseudoparticle," Phys. Rev. D **14** (1976) 3432.

[4] G. 't Hooft, "How instantons solve the U(1) problem," Phys. Rept. **142** (1986) 357.

[5] T. Schάfer and E. V. Shuryak, "Instantons in QCD," Rev. Mod. Phys. **70** (1998) 323.

[6] S. Kono, D. Jido, Y. Kuroda, and M. Harada, "The role of $U_A(1)$ breaking term in dynamical chiral symmetry breaking of chiral effective theories," PTEP **2021**, no. 9, 093D02 (2021).

[7] M. Kobayashi, H. Kondo, and T. Maskawa, "Symmetry breaking of the chiral U(3) x U(3) and the quark model", Prog. Theor. Phys., 45, 1955 (1971).

[8] E. V. Shuryak, "The role of instantons in quantum chromodynamics: (I). Physical vacuum," Nucl. Phys. B **203** (1982) 93.

[9] E. V. Shuryak, "The role of instantons in quantum chromodynamics: (II). Hadronic structure," Nucl. Phys. B **203** (1982) 116.

[10] J. J. M. Verbaarschot, "Streamlines and conformal invariance in Yang-Mills theories," Nucl. Phys. B **362** (1991) 33.

[11] Y. Suda and D. Jido, "Possible scenario of dynamical chiral symmetry breaking in the interacting instanton liquid model," Phys. Rev. D **110** (2024) 014037.

[12] K. Binder and D. Herrmann, "Monte Carlo Simulations in Statistical Physics An Introduction (6th ed.)," Springer Berlin, Heidelberg (2010).

[13] D. Randau and K Binder, "A Guide to Monte Carlo Simulations in Statistical Physics," Cambridge Univ. Press. (2014).

[14] M. Hanada, "Markov Chain Monte Carlo for Dummies," arXiv:1808.08490.

[15] J. Orear, "Least squares when both variables have uncertainties," Am. J. Phys. **50** (1982) 912, Erratum: [Am. J. Phys. **52** (1984) 278].

[16] T. Schäfer and E. V. Shuryak, "Interacting instanton liquid model in QCD at zero and finite temperature," Phys. Rev. D **53** (1996) 6522.

[17] M.A. Shifman, A.I. Vainshtein, V.I. Zakharov, "Instanton density in a theory with massless quarks," Nucl. Phys. B **163** (1980) 46.